Faculty of Electrical Engineering
Universiti Teknologi Malaysia
VOL. 10, NO. 1, 2008, 13-19
ELEKTRIKA
http://fke.utm.my/elektrika

Bandwidth Analysis of Bootstrap Transimpedance Amplifier for Optical Free Space Receiver

S. M. Idrus[1*], **S. S. Rais**[2] and **A. Ramli**[1]

[1]Photonic Technology Centre, Faculty of Electrical Engineering, Universiti Teknologi Malaysia, Johor, Malaysia.
[2]Department of Communication Engineering, Faculty of Electrical and Electronic Engineering, Universiti Tun Hussein Onn, Johor, Malaysia.

[*]Corresponding author: sevia@fke.utm.my (S. M. Idrus), Tel: 607-5535451, Fax: 607-5566272

Abstract: Free Space Optic (FSO) or optical wireless link operates in high noise environments. On the other hand, the performance is subjected to several atmospheric factors like environmental temperature, fog, smoke, haze and rain. Signal-to-noise ratio (SNR) can vary radically with the distance and ambient noise. A good sensitivity and a broad bandwidth will habitually use a small photodetection area where the aperture is small. However, FSO optical receiver requires a large aperture and accordingly, to have a large collection area, which possibly will be achieved by using a large area photodetector and large filter. Consequently, large area photodetector produces a high input capacitance that will be reduced the bandwidth. Hence, techniques to reduce the effective detector capacitance are required in order to achieve a low noise as well as wide bandwidth design. In this paper, modeling and analysis of the series and shunt with floating source: and series-shunt bootstrap transimpedance amplifier (BTA) of front-end receiver for input capacitance reduction will be presented. The result shows that the technique improved the conventional transimpedance amplifier (TIA) bandwidth up to 1000 times with an effective capacitance reduction technique for optical wireless detector.

Keywords: Bootstrap transimpedance amplifier, Free space optic, Optical receiver, Wireless optic photodetector.

1. INTRODUCTION

FSO require a large aperture and thus, the receiver is required to have a large collection area, which produces a high input capacitance that will reduce the bandwidth [1]. Photodiode capacitance can be considered as a junction capacitance of photodiode and it arises from the separation of charge in the depletion region given by

$$C_d = \frac{A\varepsilon_r\varepsilon_o}{l_d} \quad (1)$$

where A is an area of the depletion region, ε_0 is a permittivity in vacuum, ε_r is a relative permittivity of the semiconductor and l_d is a depletion region.

The total capacitance to the front-end of an optical receiver, C_{in} is given by [2]

$$C_{in} = C_d + C_s \quad (2)$$

where C_d is a photodetector capacitance and C_s is an amplifier input capacitance. We need to minimize the C_{in} in order to preserve the post detection bandwidth. On the other hand, it is necessary to reduce R_L corresponding to the following equation

$$f = \frac{1}{2\pi R_L C_{in}} \quad (3)$$

to increase the bandwidth. Consequently, the thermal noise element due to the load resistor will increase. This relationship is given by [3]

$$i_{n(Rl)}^2 = \frac{4KTB}{R_L} \quad (4)$$

where K is Boltzmann's constant, T is the absolute temperature and B is the post-detection (electrical) bandwidth of the system**.** However, typical commercial large area photodetector has capacitance around 100-300 pF compared to 50 pF in fiber link. For large detector area the C_d will increase up to 1 nF. Hence, techniques to reduce the effective detector capacitance are required in order to achieve a low noise and wide bandwidth design. Thus, in this paper the BTA is used to overcome this problem.

2. PREAMPLIFIER

There are 3 types of common preamplifier for optical wireless receiver, namely low impedance amplifier, high impedance amplifier and transimpedance amplifier (TIA). Low impedance amplifier is impractical for optical wireless receiver because it allows thermal noise to dominate within the receiver while high impedance gives improvement in sensitivity but it creates heavy demand for equalization and has a limited dynamic range. TIA is commonly used as an optical preamplifier structure, offering the best compromises in terms of noise, gain and bandwidth, all of which are influenced by the photodiode capacitance.

In this part, we review on the transimpedance front-end receiver.

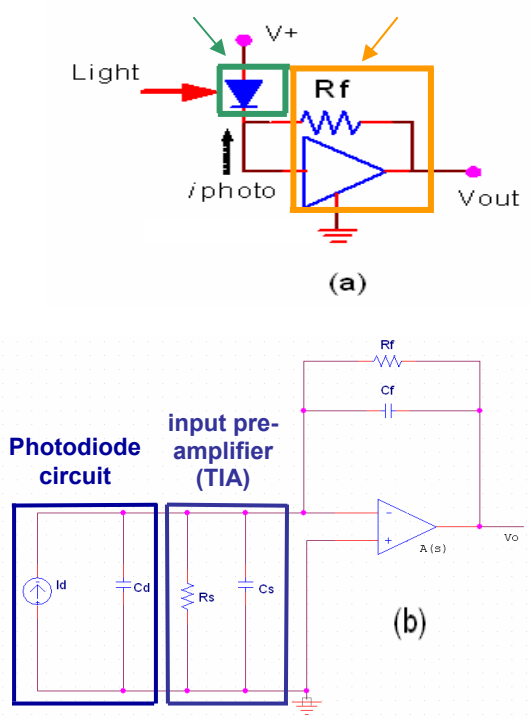

Figure 1. (a) Photodiode TIA (b) Simplified small-signal equivalent circuit of (a).

Figure 1(a) shows the photodiode with TIA, while Figure 1(b) is a simplified small-signal equivalent circuit of (a). Photodiode circuit consists of current source, i_d and photodiode capacitance, C_d. This front-end structure, acts as a current converter, gives low noise performance without the severe limitation on bandwidth forced by the high input impedance front-end design [2].

TIA using voltage feedback op-amps are widely used when a moderate/high bandwidth and a high sensitivity are necessitated. The conventional circuit shown in Figure 1 represents a virtual earth and thus almost zero load impedance to the current source. At high frequencies, the total input capacitance, C_{in} can ruthlessly limit the available bandwidth from the circuit or even cause a lightly damped/unstable dynamic response [4].

3. BOOTSTRAPPING TECHNIQUE

The basic bootstrapping principle is to employ an additional buffer amplifier to actively charge and discharge to the input capacitance as required. As a result, the effective source capacitance is reduced, enabling the overall bandwidth of the circuit to be improved. There are 2 possible bootstrap configurations (series or shunt bootstrapping modes) which can be applied to the basic circuit [4].

The shunt bootstrap circuit has an additional buffer/voltage amplifier in parallel with the main TIA while the series bootstrap circuit has an additional buffer amplifier in series with the main TIA. Figure 2 shows an example of BTA circuit arrangement of 2 types of floating source BTA (a) series BTA, and (b) shunt BTA.

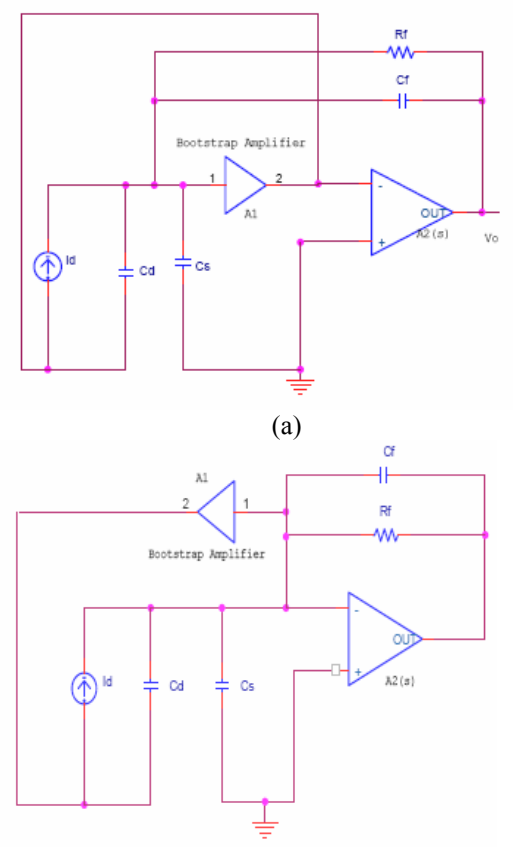

Figure 2. Floating source BTA circuit arrangement [4] of (a) series BTA, and (b) shunt BTA.

Floating source and series BTA circuit uses an additional buffer amplifier to actively charge and discharge to input capacitance as required. The effective C_{in} is reduced, enabling the overall bandwidth of the circuit to be increased. This BTA arrangement consisted of four stages. They are unity gain, FET buffer, cascade amplifier and buffer output as shown in Figure 3.

In SPICE model, the photodiode and detected optical signal was model as a current source. The transistors used in the circuit are BSX 20 - NPN bipolar transistor and BF256A - n-channel JFET depletion [1]. The photodiode and feedback capacitance are varied to observe the performance characteristics of the BTA.

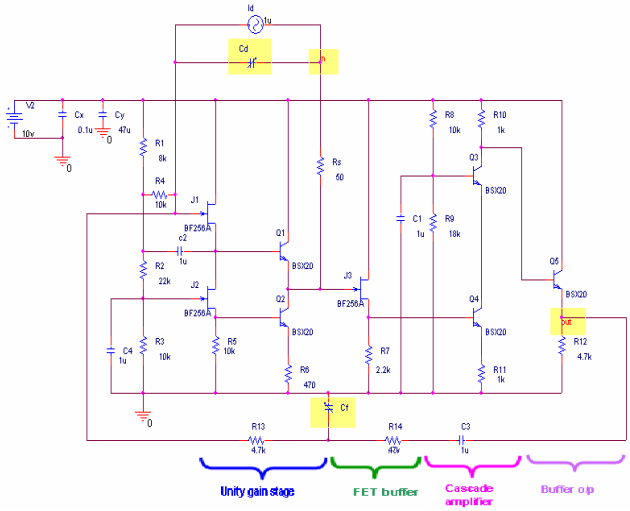

Figure 3. Floating Source and Series BTA circuit [1,8]

As SPICE is inefficient due to the limitations in modeling and plotting the optical preamplifier frequency response for different parameter, we modeled and simulated the BTA transfer function using Matlab.

The TIA gain of the circuit can be readily derived by assuming that the source resistance R_s is infinite and the op-amp has a single pole transfer function (pole frequency w_a and DC gain of A_o). The transfer function is given by [4]

$$\frac{v_0}{i} = \frac{-R_f}{\frac{s^2(C_{in}+C_f)R_f}{A_0 w_a} + s\left(C_f R_f + \frac{1}{A_0 w_a} + \frac{(C_{in}+C_f)R_f}{A_0}\right) + \frac{1}{A_0} + 1} \quad (5)$$

The source resistance was considered infinite, and the amplifiers A1 and A2 were considered to be of the same type of op-amp with a single pole transfer function where w_a is a pole frequency, w_0 is a unity gain frequency and A_0 is DC gain. The small signal transfer function of Floating Source and Shunt BTA (circuit is shown in Figure 4) is given by

$$\frac{v_0}{i} = \frac{-R_f}{M} \quad (6)$$

where M is

$$M = \frac{s^2(C_d + C_s + C_f)R_f}{\omega_0} + \frac{s(C_d + C_s + C_f)R_f}{A_0} + sC_f R_f + \frac{s}{\omega_0} - \frac{s(s+\omega_a)C_d R_f}{s+\omega_a+\omega_0} + \frac{1}{A_0} + 1 \quad (7)$$

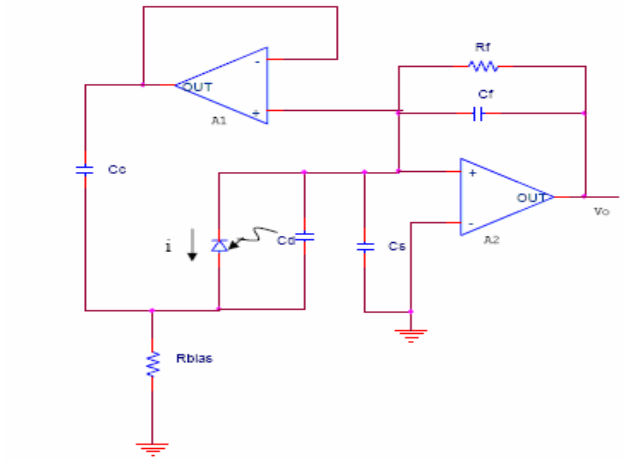

Figure 4. The schematic diagram of floating source and shunt BTA circuit

In addition, we have plotted the response of the series-shunt BTA. The circuit is shown in Figure 5 while the simplified ac model can be found in Figure 6. The transfer function can be found in Equations (8) to (17). The series-shunt BTA arrangement exploits a series-shunt positive capacitive feedback in order to compensate the "polesplitting" action of base–collector capacitance. To obtain a bootstrap action, feedback is applied to a buffered differential pair. The compensation network requires emitter degeneration resistors, R_{EE} and two capacitors in the differential pair, and does not affect biasing and low frequency behavior of the amplifier [6].

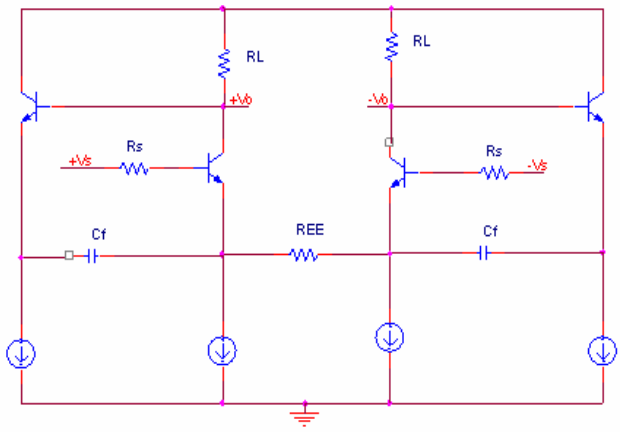

Figure 5. Series-Shunt BTA Circuit

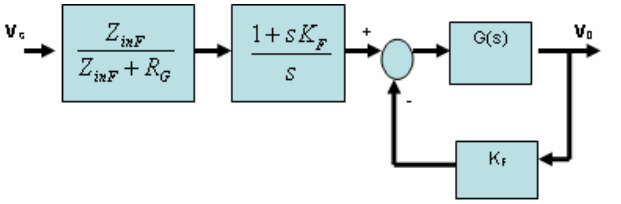

Figure 6: Simplified ac model of the shunt-series BTA circuit (Figure 5)

$$G(s) = \frac{sA_{v0}}{(1-\frac{s}{p1})(1-\frac{s}{p2})(1-\frac{s}{p3})} \quad (8)$$

$$A_{v0} = \frac{-g_m r_\pi R_L}{R_G + R_{in}} \quad (9)$$

$$p1 = \frac{R_G + R_{in}}{C_{in} r_\pi (R_G + R_E) + C_F R_E (r_\pi + R_G)} \approx \frac{R_G + R_{in}}{C_{in} r_\pi (R_G + R_E)} \quad (10)$$

$$p2 = \frac{1}{C_d R_L} \quad (11)$$

$$p3 = \frac{1}{C_F (R_G // R_E)} - \frac{1}{C_{in} (R_G // r_\pi)} \quad (12)$$

$$\beta = \frac{sC_F R_F}{1 + sC_F R_F} \quad 13)$$

$$Z_L = \frac{R_L}{1 + sC_d R_L} \quad (14)$$

$$Z_\pi = \frac{r_\pi}{1 + sr_\pi C_{in}} \quad (15)$$

$$Z_{in} = \frac{R_{in} + sr_{\pi}R_E(C_{in} + C_F)}{(1 + sr_{\pi}C_{in})(1 + sR_EC_F)} \quad (16)$$

$$\frac{Z_{inF}}{Z_{inF} + R_G} = \frac{Z_{in} - \beta g_m Z_{\pi} Z_L}{Z_{in} - \beta g_m Z_{\pi} Z_L + R_G} \quad (17)$$

4. RESULT AND ANALYSIS

The simulation results of Series BTA utilizing SPICE can be found in Figure 7 and Figure 8 in which Figure 7 is a BTA frequency responses with variable feedback capacitance, C_f and fixed photodiode capacitance, C_d = 0.1 µF. From the graph, we can see that the bandwidth and peaking gain were reduced simultaneously for lower C_f. However, Figure 8 presenting the BTA frequency responses by varying the photodiode capacitance C_d at 3.5 pF of C_f. It was shown that the bandwidth of BTA improved significantly at small C_d.

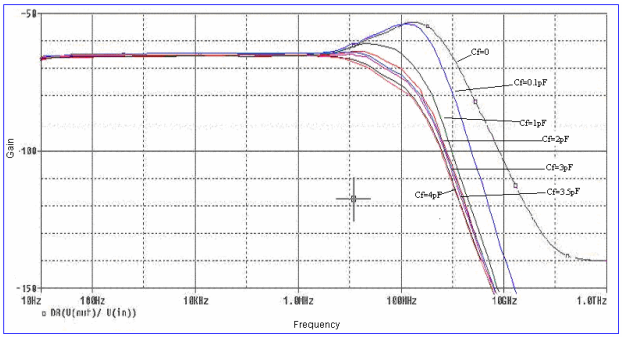

Figure 7. Simulations of BTA circuit from Figure 3 with variable C_f

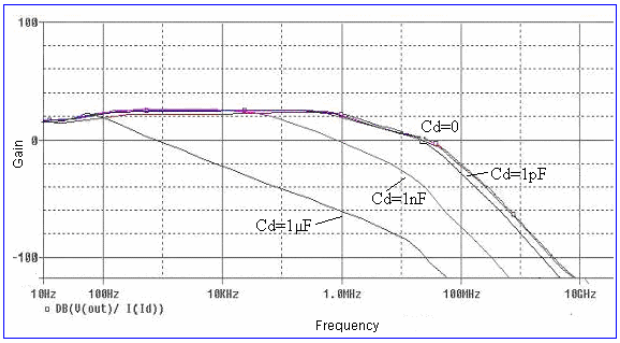

Figure 8. Simulations of BTA circuit from Figure 3 with variable C_d

From these results, we can conclude that the C_f = 3.5 pF can achieve the stable dynamic response if the C_d is fixed and equal to 0.1 µF. C_f < 3.5 pF gives the higher bandwidth than C_f > 3.5 pF but C_f < 3.5 pF will represent a lightly damped or unstable response. If this circuit is used with different photodetectors, C_d will be different. The bandwidth will reduce when C_d increase.

Simulations result for the Shunt BTA and Series-Shunt BTA utilizing MATLAB can be found from Figure 9 that shows the frequency response simulation. The bandwidth is wider than the other response when there is no C_f and C_{in} but this is impossible to achieve because photodiode capacitance is internally built-in. However, the TIA without C_f can cause the peak that represents a lightly damped or unstable dynamic response. Therefore, it needs lag compensation by introducing feedback capacitance, C_f. However, this approach does not permit the full gain-bandwidth characteristics of the op-amp to be fully exploited.

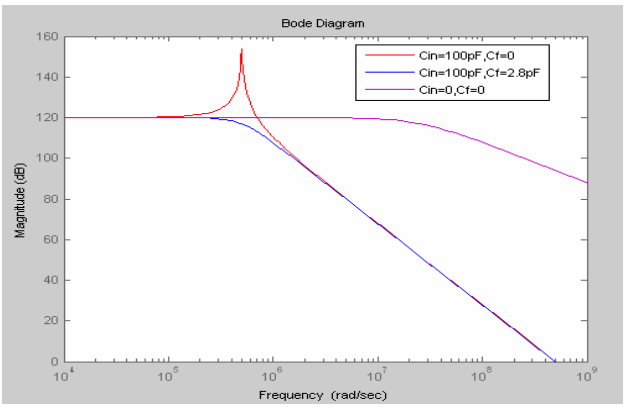

Figure 9. Comparisons of using C_f for TIA and limit case for C_{in}=0 and C_f=0

Figure 9 shows the simulation result for TIA frequency response. On the other hand, the TIA was simulated for A_0 = 50 dB by taking C_f = 2.8 pF and varying the C_d up to 1 nF as shown in Figure 10. While, Figure 11(a) and (b) expose the bandwidth and peaking gain versus C_{in} for TIA A_0 = 50 dB respectively. From these results, the frequency response shows that the C_d increases, the bandwidth reduces and peaking gain getting higher. We can also observe that C_{in} increases, the bandwidth reduces. On the other hand, C_{in} increases, peaking gain also increases. Relationship between bandwidth and C_{in} can be considered to be negative exponential while peaking gain and C_{in} to be positive exponential. Supposed in Figure 11(b), peaking gain seems positive exponential.

Table 1. Parameter used in TIA simulations

R_f	1 MΩ
A_0	50 dB
w_a	2π(40 Hz)
C_d	100-1000 pF
C_f	2.8 pF

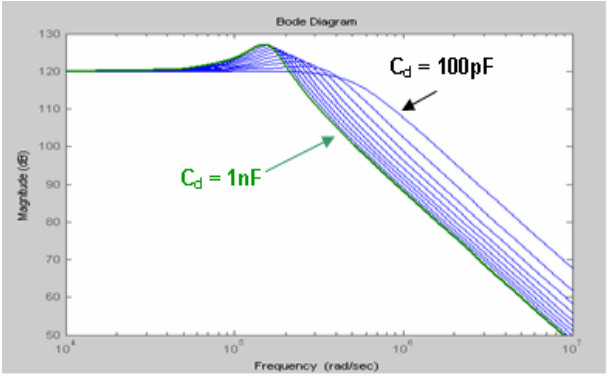

Figure 10. Frequency response of the TIA for C_f = 2.8 pF and varying the C_d from 100 pF to 1 nF.

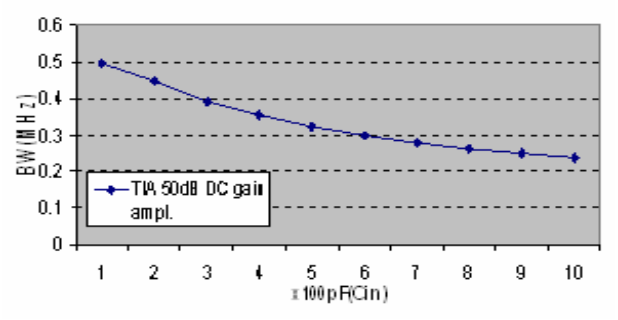

(a)

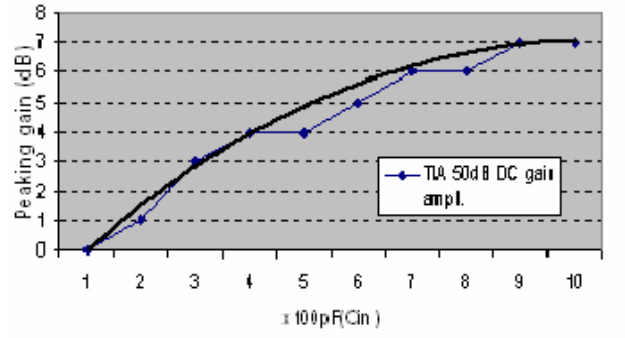

(b)

Figure 11. (a) Bandwidth versus C_{in} (b) Peaking Gain versus C_{in} for TIA $A_0 = 50$ dB

Parameters used in BTA simulations for $A_0 = 50$ dB can be found in Table 2 and its frequency response presented in Figure 12. Figure 13(a) and Figure 13(b) expose the bandwidth and peaking gain versus C_{in} for BTA respectively. By varying the C_d with fixed value of C_f, it was shown that the bandwidth decreases while peaking gain getting appears. The highest bandwidth (1.62 MHz) was archived by C_{in} = 300 pF. While the peaking gain start to appear at this total input capacitance.

Table 2. Parameter used in BTA simulations for $A_0 = 50$ dB

R_f	1 MΩ
A_0	50 dB
w_a	2π(40 Hz)
w_0	2π(40 MHz)
C_{in}	100-1000 pF
C_f	1.4 pF

Lag compensation by introducing feedback capacitance, C_f can be used to give a critically damped response. Here, we will discuss a simple method on choosing appropriate feedback capacitance, C_f. For example, for the photodiode capacitance, C_d = 500 pF with the other parameters remain, thus we need to choose higher value of $C_f > 1.4$ pF in order to reduce damping. Therefore, a frequency response of BTA for C_f was varied from 1.5 pF to 5 pF. This is shown in Figure 14. From the frequency response, we found that 1.5 pF to 2 pF is good enough to reduce damping. On the other hand, for feedback capacitance, $C_f > 2$ pF, the bandwidth will reduce simultaneously.

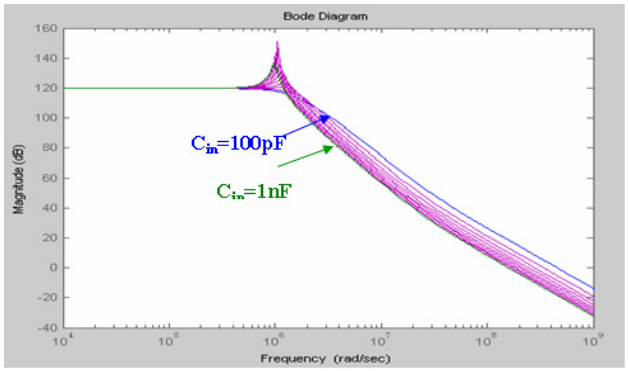

Figure 12. Frequency response of the BTA for $A_0 = 50$ dB

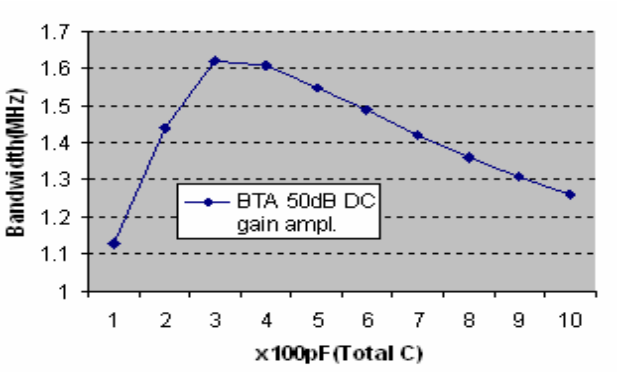

(a)

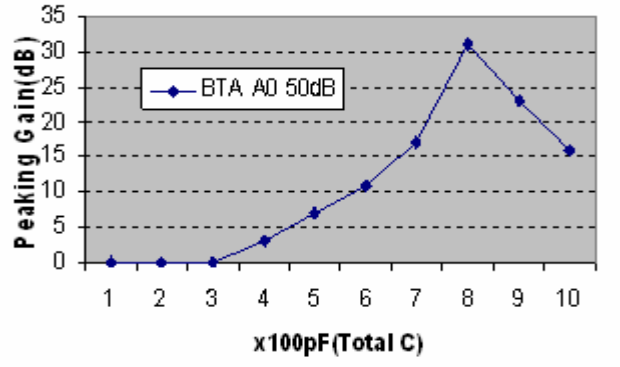

(b)

Figure 13. (a) Bandwidth versus C_{in} (b) Peaking Gain versus C_{in} for BTA with $A_0 = 50$ dB

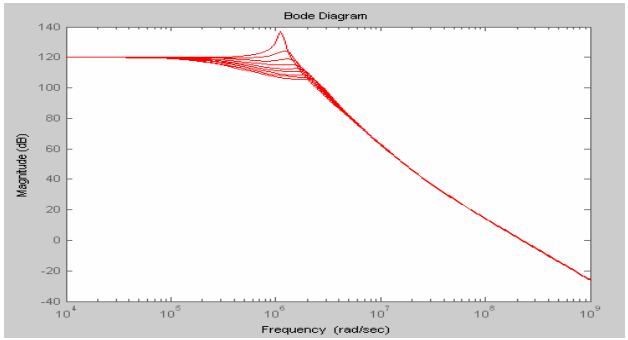

Figure 14. Frequency responses for C_f between 1.5 pF to 5 pF

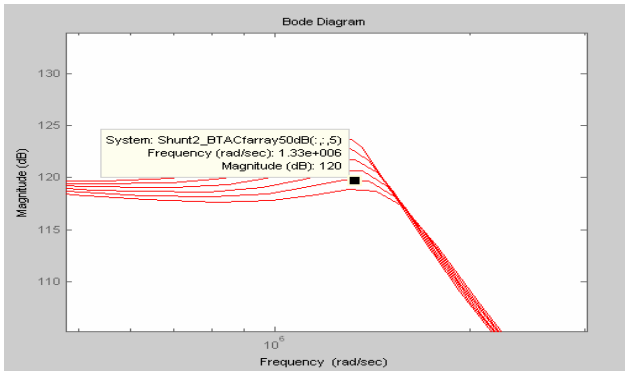

Figure 15. Frequency responses for C_f between 1.5 pF to 2 pF

Hence, from the simulation, it was found that C_f = 1.9 pF produce the same gain bandwidth product without damping as shown in Figure 15. The same technique can be applied to all C_{in} to improve bandwidth and reduce peaking gain. From the optimum C_f, the frequency response for all C_{in} can be plotted with improved system stability as shown in Figure 16. Whereby, the bandwidth decreases for C_f more than 300 pF as shown in Figure 17.

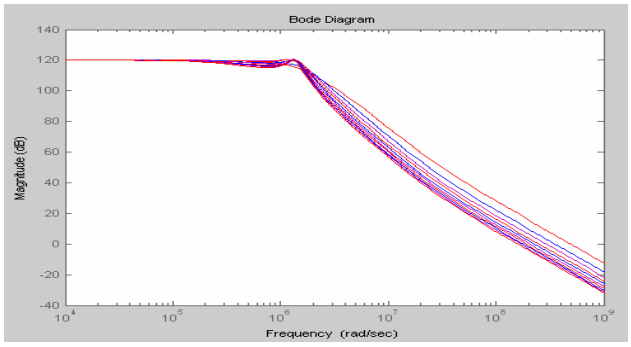

Figure 16. Stable frequency response of BTA

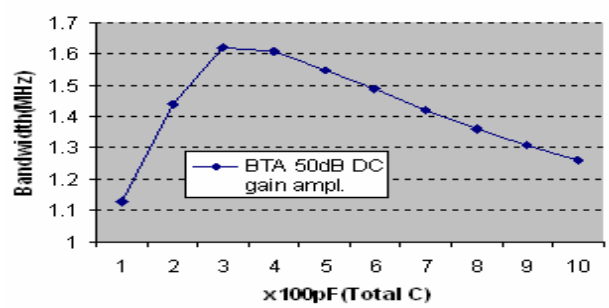

Figure 17. BTA bandwidth for varying C_{in} up to 1 nF

To compare the BTA with the conventional transimpedance front-end optical receiver, the same parameters were used to plot the frequency response of the TIA. These comparisons can be seen in Figure 18(a) and Figure 18(b) for A_0 = 50 dB and A_0 = 20 dB respectively. Thus it was shown that the designed shunt-BTA can boost the TIA bandwidth up to 1000 times higher. Even, if we used lower A_0 at 20 dB, the BTA still can produce higher bandwidth compared to TIA A_0 = 0 dB. On the other hand, the series-shunt BTA has given large bandwidth up to 982 MHz for simulation the BTA model using the following parameters; C_f = 35.5 fF, r_π = 11.2 Ω, C_d = 100 pF, R_E = 50 Ω , r_b = 164.4 Ω, R_L = 10 Ω, C_π = 31.8 fF, R_s = 100 Ω and C_μ = 15.8 fF.

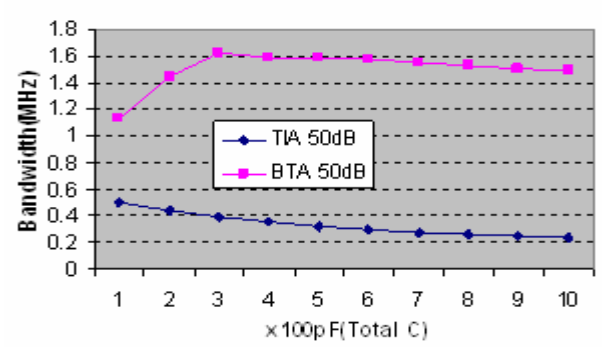

(a)

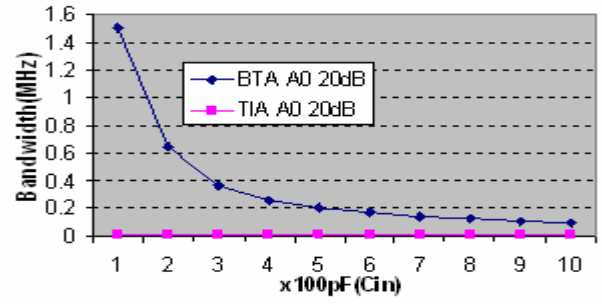

(b)

Figure 18. Comparisons between BTA and TIA (a)A_0 = 50 dB (b)A_0 = 20 dB

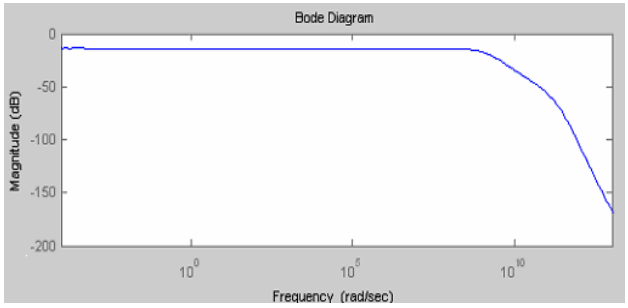

Figure 19. Series-shunt BTA frequency response for C_d = 100 pF with 3 dB bandwidth up to 1 GHz.

4. CONCLUSION

The performance of FSO is subjected to several atmospheric factors such as environmental temperature, fog, smoke, haze and rain as well as multipath induced dispersion on account of non-line of sight. Consequently, it is limiting the bandwidth to a few tens of MHz. Large area photodetectors also limits the bandwidth and SNR can vary significantly with the distance and ambient noise. Receiver sensitivity is also a very crucial parameter in developing FSO receiver.

In this paper, we address the Gain-Bandwidth product limits of amplifiers and introduce a front-end receiver that can be used to enhance the bandwidth of optical wireless pre-amplifiers with specified characteristics for their transfer function. Modeling and simulation of the Floating Source and Shunt BTA was achieved, thus improved the conventional TIA bandwidth up to 1000 times. From the presented results, we can conclude that A_0 and C_f does influence the bandwidth i.e. the BTA bandwidth is proportional to A_0. Whereby, to reduce the damping response, the C_f should be higher than C_{in} but if there is no damping, the C_f should be lower to get broad

bandwidth. Shunt-series BTA model was successfully simulated and produced bandwidth up to 1 GHz significantly for large photodiode capacitance, C_d at 100 pF.

REFERENCES

[1] R.J. Green and M. G. Mcneill, "Bootstrap Transimpedance Amplifier: A New Configuration", *IEE Proceedings*, Vol. 136, No. 2, pp. 51-61, 1989.

[2] J. M. Senior, *Optical Fiber Communications*. New York: Prentice Hall, 1992

[3] S. B. Alexander, *Optical Communication Receiver Design*. Bellingham, Washington: SPIE The International Society for Optical Engineering, 1997

[4] C. Hoyle and A. Peyton, "Shunt Bootstrapping Technique to Improve Bandwidth Of Transimpedance Amplifiers", *Electronics Letters,* Vol. 35, No. 5, pp. 369-370, 1999.

[5] S. M. Idrus, R. Ramierez-Inguiez and R. J. Green, "Receiver Amplifiers for Optical Wireless Communication System", . *3rd PREP*, University Of Keele, UK, Apr. 2001, pp. 19-20.

[6] F. Centurelli, R. Luzzi, M. Olivieri and A. Trifiletti, "A Bootstrap Technique for Wideband Amplifiers", *IEEE Transactions on circuits and systems*, Vol. 49, No. 10, 2002.

[7] R. J. Green, S. M. Idrus, R. Ramirez Iniguez and C. Sweet, "Optical Wireless Interface Technology", *OSDA Workshop*, Oundle, April 2005.

[8] S. M. Idrus, N. Hafizah and S. I. A. Azis, "Performance Analysis of Bootstrap Transimpedance Amplifier for Large Windows Optical Wireless Receiver", *RFM2006*, Putrajaya. Sept 2006.